Proceedings of the Institute of Acoustics

INVERSION AND MAPPING OF TOWED-ARRAY REVERBERATION DATA

Nicholas C. Makris and Jonathan M. Berkson

Naval Research Laboratory, Washington, D.C.

ABSTRACT Our objective is to determine the relationship between low-frequency ocean-basin reverberation data and bathymetry. Reverberation is typically measured with a horizontal towed-array. Individual monostatic observations have a 'right-left' ambiguity about the array's axis. We have developed a method for eliminating the 'right-left' ambiguity and increasing the resolution by optimal use of the data. This is accomplished by inverting multiple monostatic observations at differing array positions and orientations. We present simulations to show the superiority of this approach to data averaging, or 'stacking', which gives only qualitative results. We then present inversions performed on actual wide-area reverberation data, map the results onto bathymetry, and compare them to data stacking as a reference. Finally, we discuss the relationship between the inverted data and bathymetry.

1. INTRODUCTION

In this paper, we image portions of the western flank of the Mid-Atlantic Ridge with beamformed towed-array data acquired during the Acoustic Reconnaissance Cruise (ARC) of August 1991. Since this region is generally bottom limited with rugged bathymetry, reverberation tends to be broadly distributed in horizontal angle [1]. This poses problems in locating individual scattering features since towed-array data has an inherent "right-left" ambiguity, and has decreasing resolution for more distant returns and off-broadside beams. Averaging together scattering strength maps generated from individual reverberation observations has proven to be successful in resolving right-left ambiguity [2] [3]. However, this "stacking" technique has only been applied in situations where isolated scattering features, such as seamounts or continental margins, disturb sound channels which otherwise have excess depth. It is not expected to work as well for the broadly distributed backscattering of the ARC data. We propose an alternative imaging method based upon a global inversion of spatially distributed observations. We test this method with a simple scattering strength model using synthetic data and then apply it to real ARC data with the same observation geometry and operational parameters used in the simulation.

2. SIMULATIONS

We choose a scattering strength representation of the region to be imaged. The ocean basin is discretized into a Cartesian grid with a scattering strength assigned to each grid point. In this initial formulation we assume that scattering strength is independent of observation angle in both the horizontal and vertical. This enables us to represent scattering strength for a given region with a single image.

The image chosen to represent the ocean-basin is shown in Fig. 1. Increasing negative values indicate increasing water depth as measured from the ocean's upper surface. The data are taken from the Special Research Project (SRP) Geophysical Survey for a 244x244 km^2 region with southwest corner at 26.213° N 47.515° W [4].

INVERTING TOWED-ARRAY REVERBERATION

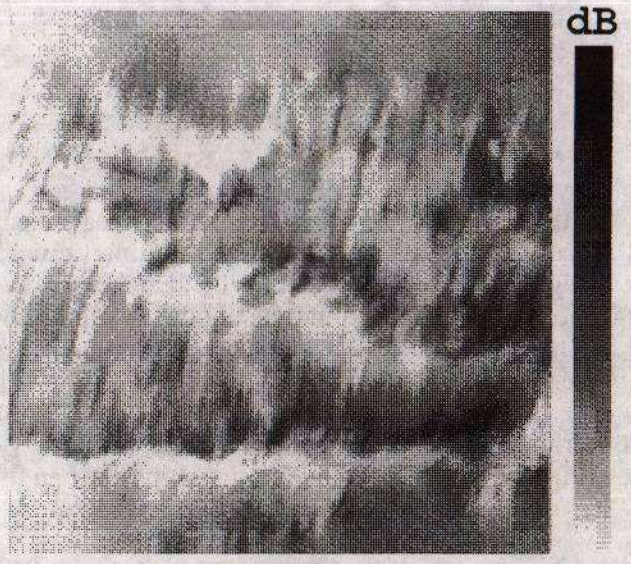

FIG. 1

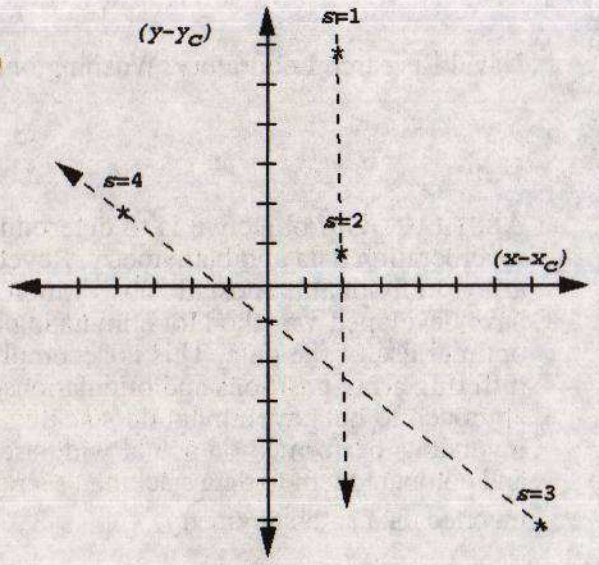

FIG. 2

For the simulations, scattering strength, $\Sigma[m,n]=10\log(\sigma[n,m])$, is chosen to be equal to the value of depth, in hundreds of meters, for respective east vs. north grid point coordinates $m=1,2,3,...,N_X$ and $n=1,2,3,...,N_Y$, originating at the southwest corner of the region to be imaged, where $N_X=N_Y=163$. This serves two purposes. It defines scattering strength values which fall within the range typically measured and, it defines a scattering region which has variations related to the bathymetry. Linear scatter coefficient is given by $\sigma[n,m]$.

The synthetic observation geometry, with towed-array course, is indicated in Fig. 2. The coordinate axis shown is at the center of the region displayed in Fig. 1, ie at $m_C=x_C/\Delta r=81$, $n_C=y_C/\Delta r=81$, where $\Delta r=1.5$ km. Monostatic observation locations are given by asterisks. Array axis orientations are within +/- 5^o of the tracks shown, in accordance with experimental deviations.

To compare observations from various array positions and orientations, reverberation must be mapped in space. For real data, temporal returns measured on an array of hydrophones can be accurately converted to range and azimuth. Beamforming yields the necessary azimuthal dependence, but with varying resolution and right-left ambiguity. Travel-time can then be linearly converted to range, via mean sound speed, with high accuracy for ranges larger than a few ocean depths. More complex conversions using slant-range or ray travel-time are necessary for local returns. For synthetic data, however, it is possible to maintain a spatial representation throughout.

Reverberation measured a distance r from the array, at angle θ from its axis, is comprised of returns weighted over azimuth and integrated within an annulus of width $\Delta r=c\tau/2=1.5$km, where c is the mean sound speed, and τ the pulse duration for cw signals. The azimuthal weighting is determined by the array's beampattern in the θ direction. In our inversion and simulations, we ignore the contribution from side-lobes in the beampattern, and approximate the azimuthal weighting by unity within the 3dB beamwidth $\beta(\theta)$ and zero outside. The resulting integration region is an annular sector of area $r\beta(\theta)\Delta r$ centered about the point (r,θ). Contributions from a symmetric annular sector centered at $(r, -\theta)$ are also added, to account for the array's right-left ambiguity. To generate synthetic reverberation maps Q_S, scatter coefficients at grid points within

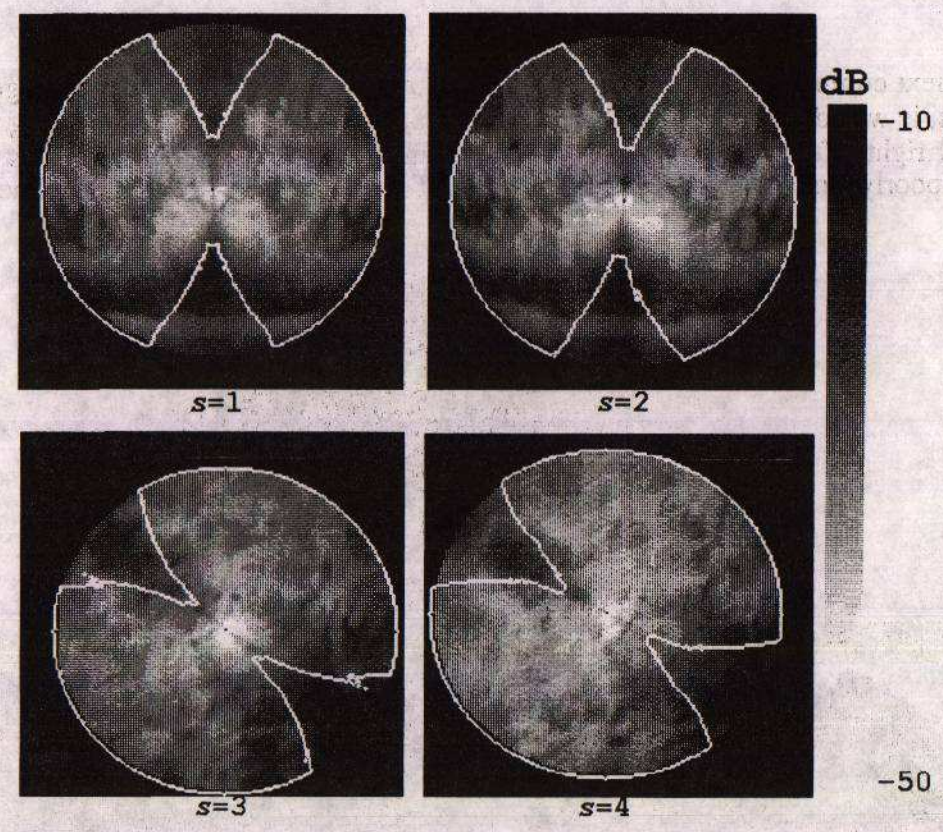

FIG. 3

ambiguous annular sectors are weighted by transmission loss, taken to be zero in these simulations, and summed together incoherently [5].

Synthetic reverberation maps $10\log(Q_S)$ for the s=1,2,3,4 observations are shown in Fig. 3. All data to be used for scatter coefficient estimation are within the exterior white line, ie poor resolution data from endfire beams and beyond a threshold range are excluded.

Due to thresholding, the mapping $Q_S[n,m]$ may not exist at a given grid point $[n,m]$ and observation s. To quantify this for the chosen observation geometry, the number of mappings per grid point Ω is shown in Fig.4.

We first show the scattering coefficient estimate resulting from a linear average of reverberation maps. We add all mappings Q_S for a given grid point and divide by the number of mappings for that grid point. The resulting scattering coefficient estimates $\hat{\sigma}[m,n]$ are converted to scattering strengths via $\hat{\Sigma}[m,n]=10\log(\hat{\sigma}[m,n])$, for $m=1,2,3,...,N_x$, and $n=1,2,3,...,N_y$. The resulting image, in Fig. 5, bears a poor resemblance to the actual scattering strength image in Fig. 1. In general, the magnitude and shape of estimated scattering features are significantly different from the actual ones. Artificial features of high scattering strength also appear due to imperfect resolution of right-left ambiguity.

We next compute the scattering strength estimate resulting from a dB average of reverberation maps, ie we add all mappings $10\log(Q_S)$ and again divide by Ω. The resulting image, Fig. 5, has better right-left ambiguity reduction than the linear estimate, but still resembles the original image only poorly, and the mean estimate is orders of magnitude worse than in the linear average.

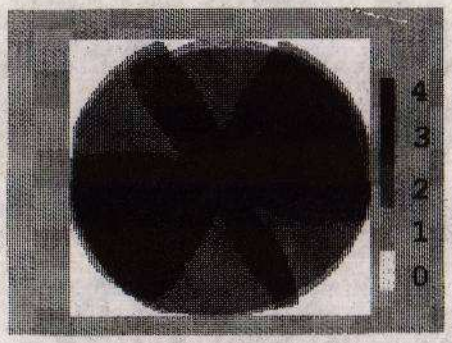

FIG. 4

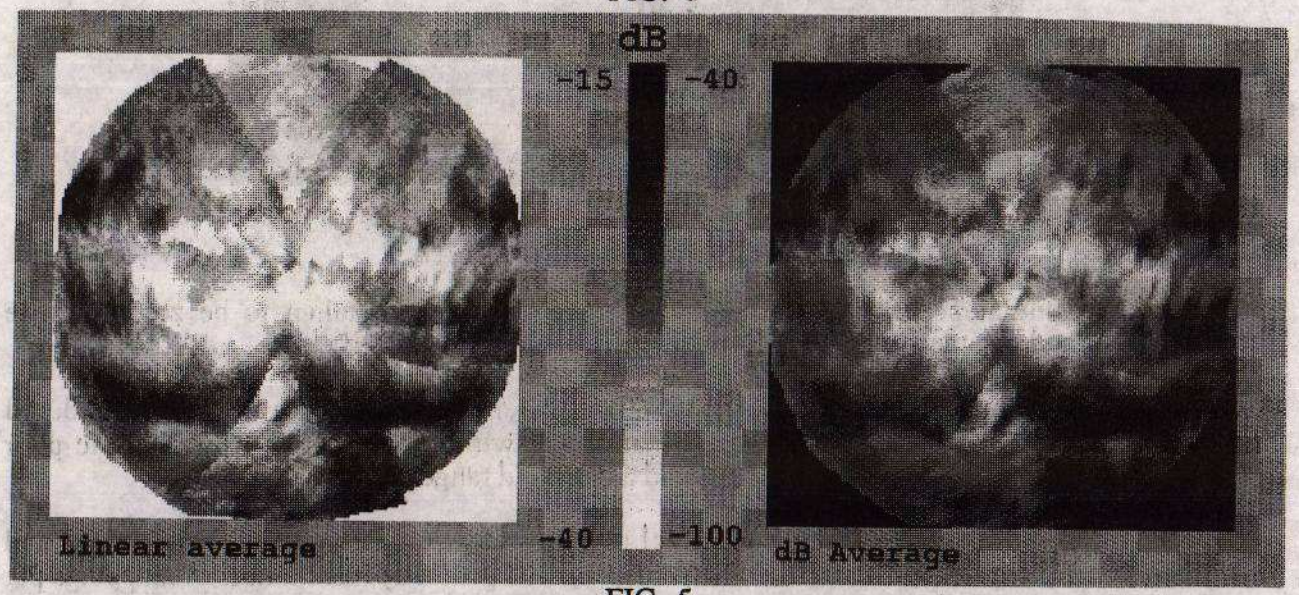

FIG. 5

To perform a global inversion we initialize our scattering coefficient estimate $\hat{\sigma}[m,n]$ at some value within an allowable range $\sigma_{min} < \hat{\sigma}[m,n] < \sigma_{max}$ for all grid points $m=1,2,3,..N_X$ and $n=1,2,3,..N_y$. We construct replica data $R_S[m,n]$ in the same way that synthetic data was constructed, but use the estimated scattering coefficient $\hat{\sigma}[m,n]$ in place of the actual scatter coefficient $\sigma[m,n]$. We then compute a cost function which sums the difference squared between replica data and true data for each observation and grid point

$$E(\hat{\sigma}) = \sum_{s=1}^{S}\sum_{m=1}^{N_x}\sum_{n=1}^{N_y}\left(R_s[m,n] - Q_s[m,n]\right)^2$$

We perturb our estimated scattering coefficient at a single grid point, and recompute the cost function. If the cost function E' including the perturbation is less than the original cost function E we accept the perturbation. Otherwise we retain the original value. We continue this process for each grid point. That comprises the first global iteration. We then iterate globally until the cost function reaches a minimum value, E_{min}, with respect to the $\hat{\sigma}[m,n]$. This method is equivalent to the gradient method since the cost function can only decrease or remain constant. Since the problem may ultimately be written as a set of coupled linear equations, ie the cost function is parabolic in the varied parameters, the local minimum obtained by the gradient search is the global minimum [5].

The scattering strength estimate for the global inversion is shown in Fig 6. It is identical to the original image, Fig. 1. The right-left ambiguity of the data has been removed and the image is resolved to one pixel in regions where reverberation mappings of such high resolution do not exist. The mean values are also identical. (Some grid points in the periphery of the image are not properly estimated due to insufficient information. To distinguish these, a light line in the figure encompasses grid points where $1<\Omega$.)

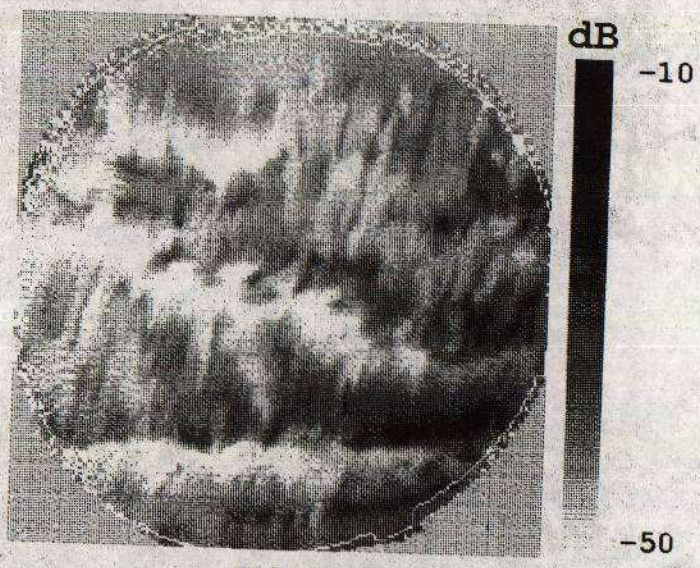

FIG. 6

3. MID-ATLANTIC RIDGE REVERBERATION DATA

We next examine actual reverberation data measured in the same region specified in Fig. 1 with the observation geometry of Fig. 2. Since we will be mapping reverberation onto bathymetry in all subsequent plots, we first give an example of the bathymetric elevation as seen with Lambertian shading from a source at infinity centered above our region, Fig 7. An actual ARC reverberation map corresponding to observation s=2 in Fig. 2 is also shown in Fig. 7. The τ=2 s cw pulse is centered at 270 Hz and emanated from a 10 element vertical line array of 60 m length centered at 165 m depth. It was received by an evenly spaced 64 element towed-array of 160 m length.

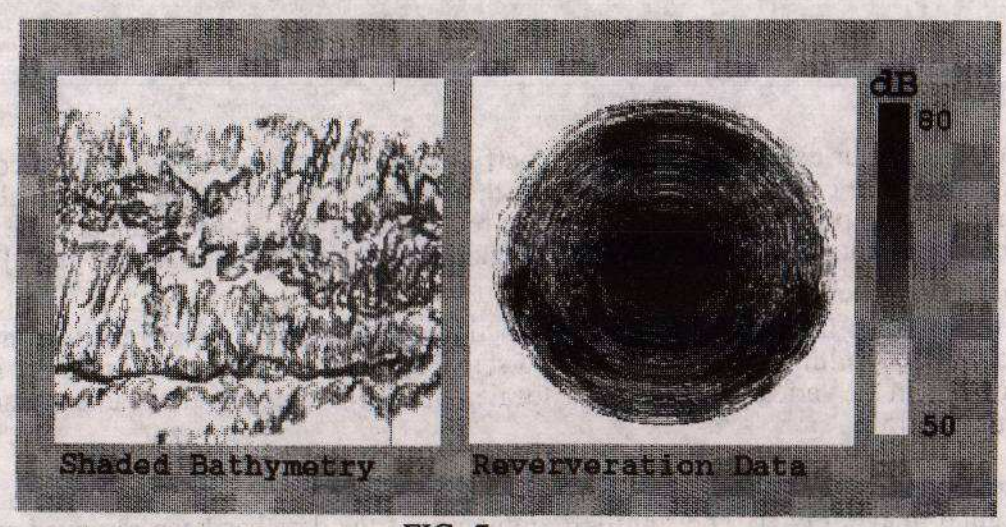

FIG. 7

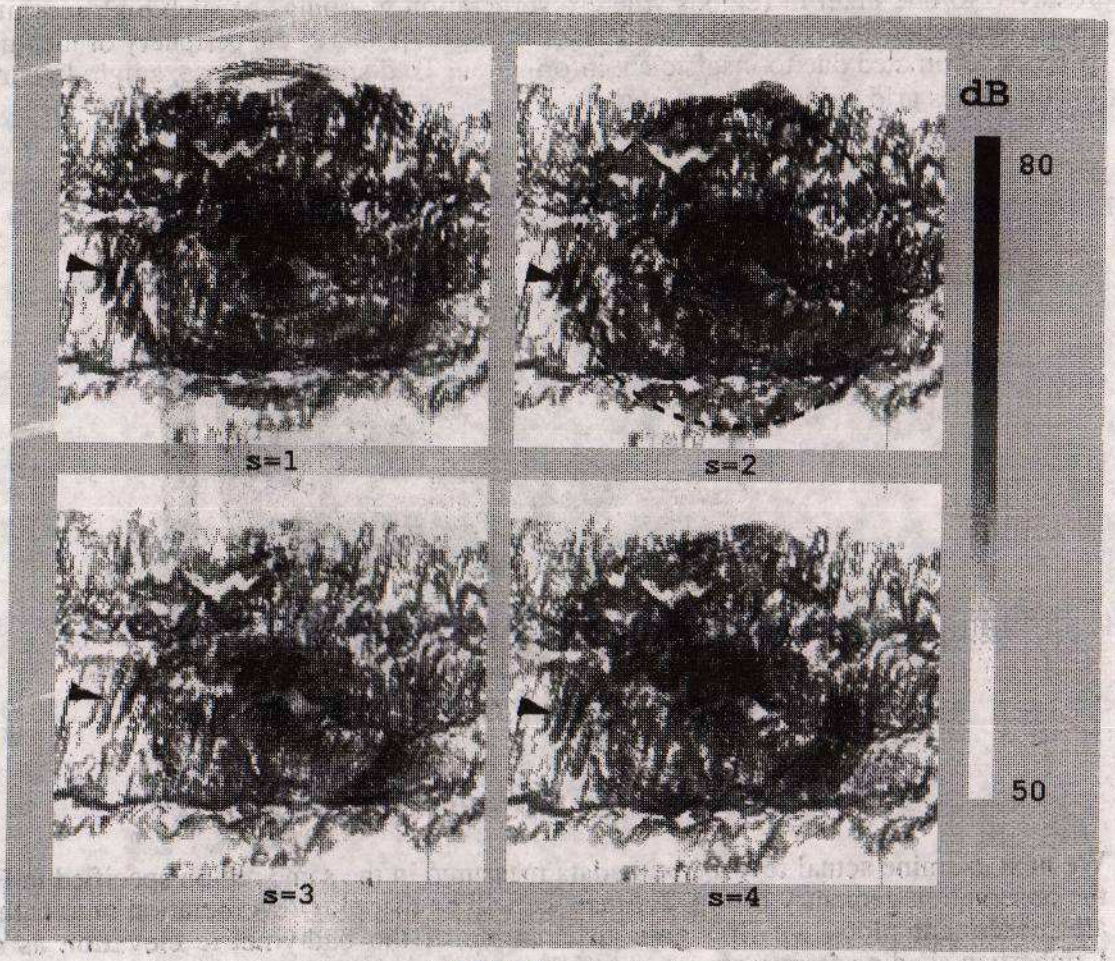

FIG. 8

In Fig. 8 we map reverberation directly onto the Lambertian shaded bathymetry, originally done in color. For s=2 two concentric circles indicate the bottom bounce convergence zones (cz) at roughly 30 km and 90 km from the source, ie .5 cz and 1.5 cz. We further note that due to bottom limitation for depths shallower than the conjugate depth 3900 m, reverberation at 1.5 cz is limited

to two free azimuths which intersect the deep east-west rift valley where it intersects the first ray vertex at .5 cz from the respective source. A prominent bathymetric feature is shown with an arrow in each map. When the feature is 1.5 cz from a given source and is also at a free azimuth, a strong return is mapped there, as in s=1,2,4. However, all of these maps still have right-left ambiguity, and ambiguous returns also appear in the rift valley where bottom interaction is not anticipated.

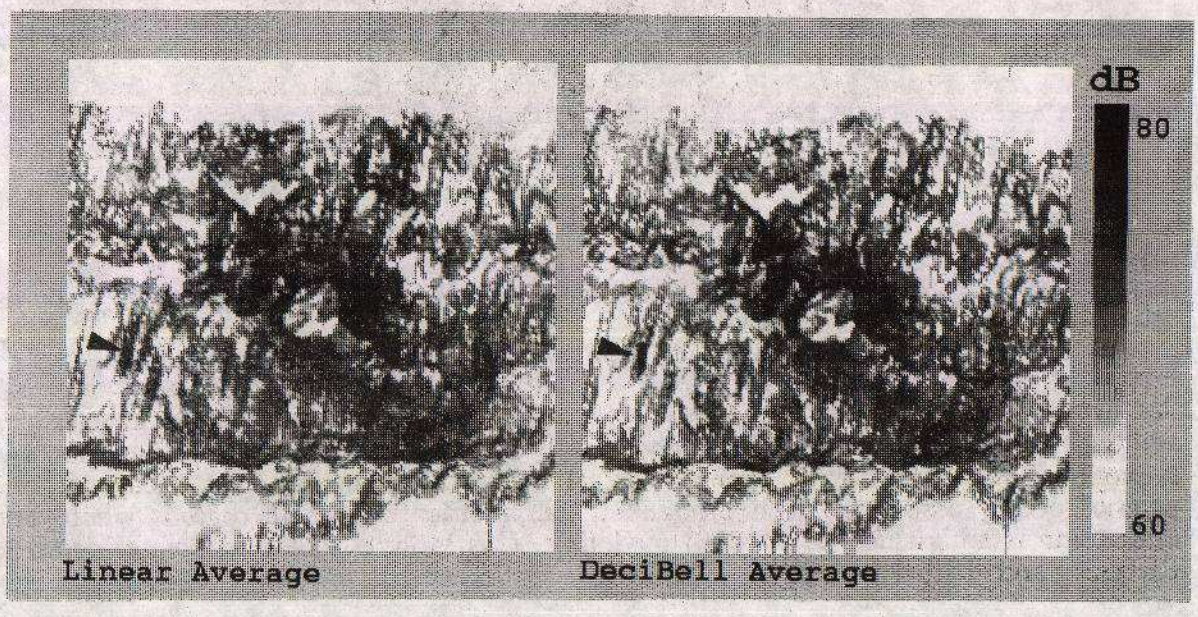

FIG. 9

We have combined the maps in Fig. 8 via linear and dB averaging to produce the reverberation estimates found in Fig 9. We note that right-left ambiguity is still apparent in both of these estimates. (We do not use data within .5 cz due to error in the linear mapping procedure used.)

We have also performed a global inversion. The result is shown in Fig. 10. A strong return can be unambiguously identified with the ridge previously marked. Reverberation is also distributed about bottom limited regions, and generally coincides with prominent features, but is not found in regions which exceed conjugate depth, such as the rift valley.

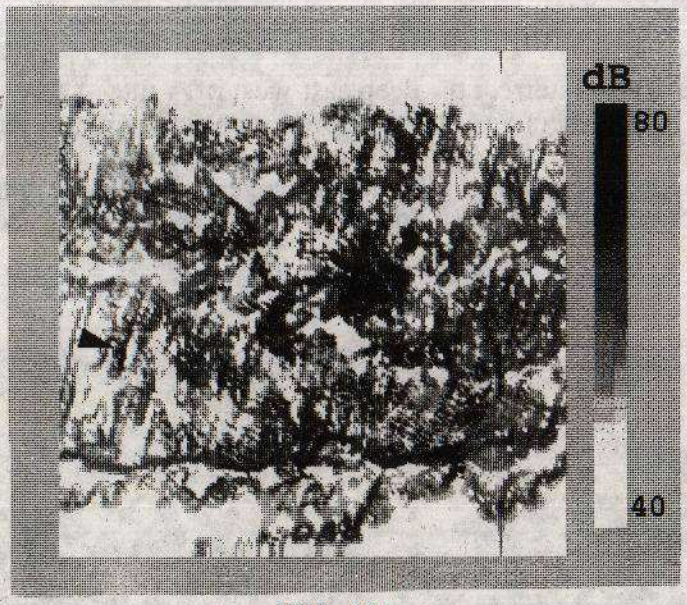

FIG. 10

4. CONCLUSIONS

We have applied an inversion method which optimizes resolution and removes right-left ambiguity in towed-array reverberation data. The method has been shown superior to data averaging in simulations. When applied to actual reverberation data, strong backscatter returns are unambiguously associated with prominent bathymetric features in regions where bottom interaction is anticipated by forward modeling. This is investigated in greater detail in an upcoming article [6].

5. REFERENCES

[1] J.M. Berkson, N.C. Makris, R. Menis, T.L. Krout and G.L. Gibian, 'Long-range measurements of sea-floor reverberation in the Mid-Atlantic Ridge area,' in *Ocean Reverberation*, edited by D. Ellis, J. Preston and H. Urban (Kluwer, Dordrecht) (1993).

[2] F.T. Erskine, G.M. Bernstein, S.M. Brylow, W.T. Newbold, R.C. Gauss, E.R. Franchi and B.B. Adams, 'Bathymetric Hazard Survey Test (BHST Report No. 3), Scientific Results and FY 1982-1984 Processing,' NRL Report 9048 (1987).

[3] J.R. Preston, T. Akal and J.M. Berkson, 'Analysis of backscattering data in the Tyrrhenian Sea,' J. Acoust. Soc. Am. *87*, 119-134 (1990).

[4] The Special Research Program on bottom reverberation is Office of Naval Research sponsored and involves a number of joint acoustic and geophysical experiments in the MAR.

[5] N. C. Makris, 'Imaging Ocean Basin Reverberation via Inversion,' paper submitted to J. Acoust. Soc. Am.

[6] N. C. Makris and J. M. Berkson, 'Inverting, Imaging and Mapping Mid-Atlantic Ridge Reverberation onto Bathymetry,' paper submitted to J. Acoust. Soc. Am.